

Investigation on the combined Rankine-absorption power and refrigeration cycles using the parametric analysis and genetic algorithm



Soheil Mohtaram, Wen Chen*, Ji Lin

Institute of Soft Matter Mechanics, College of Mechanics and Materials, Hohai University, Nanjing 210098, China

ARTICLE INFO

Keywords:

Combined cycle
Absorption cycle
Ammonia-water mixture
Genetic algorithm
Refrigeration cycle

ABSTRACT

This study investigates the combined Rankine power and the absorption cooling cycles. The working fluid used in this cycle is the binary liquid mixture of water and ammonia. It produces both refrigeration and power simultaneously via a single heat source. Parametric analysis has been adopted to evaluate the thermodynamic parameters effects on the operation of the combined cycle where the Engineering Equation Solver (EES) is utilized. The obtained results show that environmental temperatures, heat source, refrigeration, inlet pressure, and temperature, and the density of the ammonia-water dilution have major effects on the exergy efficiency, the refrigeration output, and the net power of the system. In order to obtain the maximum exergy and thermal efficiencies, the optimization of the combined cycle has been performed via the genetic algorithm.

1. Introduction

In recent decades, a large amount of wasted heat has been released to the environment in the form of exhaust gases from turbines and engines [1]. Therefore, there is a growing trend to use the binary mixtures instead of Chlorofluorocarbons (CFCs) in gas cycles due to the global warming and its corresponding environment problems [2,3]. The application of binary mixtures such as the ammonia-water and/or the lithium-bromide [4] instead of the CFCs can help to mitigate the global warming.

In Ref. [5], the mixture of ammonia and water was first taken as the working fluid of an absorption cooling cycle to study whether it would afford high thermal efficiencies than these obtainable from a comparable steam power cycle. At the same time, the condensation process is performed at various temperatures to create more pressures than those for the conventional Rankine steam turbines. This high pressure is satisfied in order to preclude the air from entering the system, but is not favorable for the power production and the efficiency of the cycle. And then a power cycle was proposed to employ the mixture of ammonia-water as the operator fluid of the lower cycle [6]. The high-pressure problem in the cycle is solved by the replacement of the condensation process with an absorption process [7]. The combined refrigeration and power thermal cycle has been proposed by Goswami [8]. After that, other researchers have worked on the efficiency of this cycle [9,10]. Yang et al. [11] proposed a new combined power and ejector-refrigeration cycle and conducted the combined cycle analysis for zeotropic mixtures to illustrate effects of fluid compositions and working

conditions. Mohtaram et al. [12,13] made detailed energy exergy analysis to find the effects of compressor pressure ratio and ammonia-water dilution on a combined cycle via the EES software. Ahmadi et al. [14] conducted many researches on power plants and combined cycles. They selected Shahid Montazeri power plant in Iran and firstly investigated all cycle equipment. The EES software was utilized for such analysis. In their study, Condenser was the main equipment to waste exergy. They also investigated the feed water heating of the power plant [15] and proposed energy efficiency and exergy destruction as the objective functions. The Cycle tempo software was used for the analysis conducted in these two cases: low pressure and high pressure heart recovery. They made a further investigation on Montazeri power plant on evaluating a full repowering with merging solar energy [16], in which a 400 MW gas turbine for full repowering and solar energy is used for evaporating a part of feed water in parallel with HRSG. Annual effects on fuel consumption, decrease in CO₂ emission, and pressure levels of HRSG on cycle performance are evaluated. Then, they evaluated the use of solar thermal energy for heating parallel feed water in repowering Montazeri power plant [17].

By replacing all high-pressure feed water heaters with solar collectors [18], exergy efficiencies and net energy increased by 9.5% compared with the simple cycle, reaching 35.21% and 36.85%, respectively. Keshavarz et al. [19] modeled the industrial scale reaction furnace of Ilam gas treating plant by 3D computational fluid dynamics (CFD). They found that Oxygen and acid gas at center tend to swirl when encountering blades of air and acid gas diffusers. Akbari et al. [20] investigated the effect of semi-attached rib on heat transfer and

* Corresponding author.

E-mail address: chenwen@hhu.edu.cn (W. Chen).

Nomenclature		E_{in}	exergy of heat source fluid
P	pressure (MPa)	Q_{in}	total heat added to the cycle
t	temperature (°C)	<i>Subscripts and superscripts</i>	
T	temperature (K)	B	boiler
Q	heat transmitted (kW)	C	condenser
W	power (kW)	eva	refrigeration output
S	entropy (kJ/kg K)	eva,i	evaporator inlet
h	enthalpy (kJ/kg)	eva,o	evaporator outlet
g	heat resource	i, j, k, l	state points
x	density of ammonia dilution	0	environment state
x_i	mass fraction of components	eva, j	evaporator
m	mass flow rate	rec	rectifier
η_1	first low efficient	Ph	physical
η_2	second low efficiency	Ch	chemical
η	efficiency	<i>imf</i>	initial mass fraction
E	total energy (kJ/S)	<i>vmf</i>	vapor mass fraction
U	internal energy		

liquid turbulent flow [21] of Nano fluid [22] water–copper oxide in three-dimensional rectangular microchannel. The numerical results are compared with those of smooth channel.

Since this combined cycle applies the high-density ammonia gas for power generation in turbine, the gas passes through heat exchanger after the turbine exhaust, and meanwhile losses the sensible heat which is needed for chilling water. Consequently, the output of refrigeration is comparatively minuscule [23]. In order to yield greater refrigeration outcomes, the fluid is required to change phases in cooler [24]. Zheng et al. [25] proposed an absorption power/cooling combined cycle, in which the thermodynamic analysis of cycle is performed by using log p–T, log p–h and T–s diagrams. Their considered cycle was based on the kalina cycle [26–28] where a rectifier is used to provide higher densities of ammonia water vapour for the cooling. The evaporator and condenser are placed between the second absorber and the rectifier. With these changes, the cycle is capable to produce more refrigeration and power. Zhang et al. [29] suggest a novel ammonia water cycles for the combination of power and refrigeration. They employ an absorbent separator in their investigations. As a result, new cycle is introduced in [30,31] for the simultaneous production of refrigeration and power which employs the mixture of water and ammonia as the operator fluid. By using this working fluid, high energy and exergy efficiency are achieved for their considered cycles. Although these cycles results in high efficiencies, but they are quite complicated and involve high costs in terms of investment. Wang et al. [32] present a refrigeration and

power cycle which is a combination of the Rankine cycle and the absorption refrigeration cycle, and high exergy efficiency is obtained for this cycle. Pouraghaie et al. [33] proposed a combined thermal power and cooling cycle where thermal energy was used to produce work and to generate a sub-ambient temperature stream. The main purpose of their research was to employ multi-objective algorithms with Pareto approach optimization of thermodynamic performance of the cycle. The main conflicting thermodynamic objective functions considered in their investigation was turbine work, thermal efficiency and cooling capacity. It was shown that some important relationships among optimal objective functions and decision variables involved in the combined cycle can be recognized from this study. Joachim-André Raymond Sarr and François Mathieu-Potvin [34] conduct a theoretical analysis in order to increase the thermal efficiency of Rankine cycles by using a refrigeration cycles by connecting it to a refrigeration cycle. Their idea is to use the refrigeration cycle to create a low temperature heat sink for the Rankine cycle.

As shown in Fig. 1, the cycle considered in this study combines the Rankine power cycle with the absorption cooling cycle to be capable of producing both power and refrigeration with the use of a single low temperature heat source such as solar or geothermal energy. Due to the feature of the considered structure, the internal functioning parts as well as assumed optimum conditions of this cycle, it is capable of producing higher refrigeration output which is related to other refrigeration and power cycles. Heretofore, the exergy efficiency of

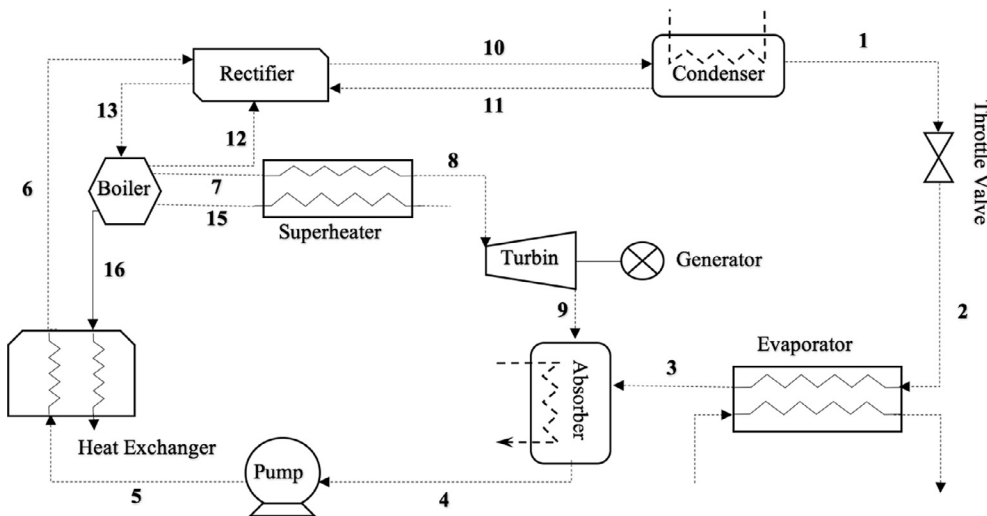


Fig. 1. The considered schematic diagram of the combined power and refrigeration cycle.

combined cycle is investigated. In addition to maximize exergy efficiency, we calculate the maximum net power output of refrigeration, the maximum output of net power, and the maximum thermal performance. The Engineering Equation Solver (EES) software is used for parametric analysis of the thermodynamic parameters effects on the performance of considered combined cycle. The cycle is then optimized by the genetic algorithm for obtaining the maximum exergy efficiency and refrigeration load.

2. Cycle descriptions and assumptions

It is pre-supposed that the considered system has achieved a stable state where the pressure drop and the heat losses inside the pipelines can be neglected. Enriched mixture of ammonia in evaporator's outlet is at saturated state. It can be added that, in aqua-ammonia refrigeration systems, the ammonia is the refrigerant, and the water is the absorbent, and the vapor produced in the generator contains minor fraction of water [35]. The minimum pressure of system is rectified by considering the absorber outlet temperature. The density of the base dilution is numerated by the absorber pressure and temperature. The exit temperature of the absorber (inlet of pump) is supposed at an approximate 5 °C above the ambient temperature. Exiting enriched ammonia vapor from the rectifier is assumed as saturated vapour and the weak outlet dilution is assumed to be saturated fluid. Condenser output is also saturated fluid and its temperature is assumed to be 5 °C higher than the ambient temperature.

The considered cycle in this study as shown in Fig. 1 is used where a saturated base dilution leaves the absorber towards the pump (path 4) and its pressure is increased by the pump (path 5). Then, it is heated by the heat exchanger via the path 6 and is finally sent to the rectifier. Inside the rectifier, it is divided into two streams: the enriched ammonia vapor (path 10) and the weak ammonia dilution (path 13). A heater is located under the rectifier where the weak dilution of ammonia-water is heated and turns into the saturated vapor (path 7). The weak saturated dilution is heated by the super heater and is sent to the turbine (path 8). The enriched ammonia vapor is converted into liquid inside the condenser after passing through a pressure relief valve; and its pressure is reduced (paths 1 and 2). This path that is always unalloyed ammonia is entirely converted into vapor by the evaporator (path 3). And this stream is then absorbed by the absorber using the weak dilution from path 9 that has been expanded inside the turbine.

Again, the basic dilution of ammonia water is formed which completes the cycle. The heat source fluid is first passed through the super heater (path 14) and then via path 15 enters the steam boiler. It then passes through the path 16 and goes to the surroundings after passing the heat exchanger via path 17.

3. Thermodynamic and parametric analysis

3.1. Thermodynamic pattern

For obtaining the efficiency of the combined refrigeration and power cycle, fluid states in different points have to be taken into account. In this section, different relationships for each fluid state within the cycle parts are evaluated. The cycle under study contains main equipment such as the heat exchanger, the turbine, the pump, the boiler, and the pressure relief valve that are combined with comparatively complicated equipments suchlike, rectifier, condenser and absorber. Each part of the cycle can operate like a volume control unit with the existence of a working fluid responsible for heat transfer. The overall energy and mass balances of the cycle are as follows:

$$\Delta \left(\sum_{out}^{in} m_i \right) = 0 \quad (1)$$

$$\Delta \left(\sum_{out}^{in} m_i \cdot h_i \right) + \Delta \left(\sum_{out}^{in} Q_j \right) + \Delta \left(\sum_{out}^{in} W_k \right) = 0 \quad (2)$$

Additionally, refrigerant mass expression is valid in the absorber and rectifier.

$$\Delta \left(\sum_{out}^{in} x_i \cdot m_i \right) = 0 \quad (3)$$

3.2. Calculation and analysis of considered combined cycle

In this section, analysis of different modes of the working fluid at different stages as presented in Figure should be discussed.

3.2.1. Path 4 (pump's inlet)

In the absorber, it has been assumed that the mixture keeps in the saturated state. The minimum pressure and temperature of the absorber is used for determination of density level of base dilution. The outlet temperature of the absorber is considered to be 5 °C higher than the ambient temperature. The reference flow rate is assumed at this stage, and all other flows inside the system are a ratio of this reference flow rate. At this stage, the pressure considered as minimum possible pressure and the mass flow rate is equal to the reference flow rate. In addition, the density is proposed as the density of the base dilution.

$$T_4 = T_0 + 5 \quad (4)$$

$$P_4 = P_{min} \quad (5)$$

$$x_4 = \text{The density of the base dilution} \quad (6)$$

$$m_4 = \text{Reference flow rate} \quad (7)$$

3.2.2. Path 5 (Pump outlet)

The pump is used to increase the pressure of the base dilution. And then, the considered pressure could be in its maximum statue. By obtaining the isentropic factor of the pump, pressure and enthalpy can be easily calculated

$$P_4 = P_{max} \quad (8)$$

$$S_{isentropic} = S_4 \quad (9)$$

$$x_5 = x_4 \quad (10)$$

$$m_5 = m_4 \quad (11)$$

$$m_{pump} = m_4 \times (h_5 - h_4) \quad (12)$$

$h_{isentropic}$ enthalpy of the pump outlet stream for compression under isentropic conditions is calculated.

$$\eta_{pump} = \frac{h_5 - h_4}{h_{isentropic} - h_4} \quad (13)$$

3.2.3. Path 6 (heat exchanger's outlet stream and inlet of rectifier)

The temperature of the base dilution is increased after heated by the heat exchanger. In this state mass flow rate and density of ammonia dilution are equal to those of the state 4, and the temperature is 15 degree less than the outlet temperature of boiler. Conditions under the state 6 are as follows:

$$T_6 = T_{16} - 15 \quad (14)$$

$$P_6 = P_5 \quad (15)$$

$$x_6 = x_4 \quad (16)$$

$$m_6 = m_4 \quad (17)$$

3.2.4. Path 10, 11, 12 and 13 (input and output of rectifier)

The base dilution reaches the rectifier after passing through the heat exchanger. Inside the rectifier, the following relationships hold:

$$\Delta \left(\sum_{out}^{in} m_i \right) = 0 \quad (18)$$

$$\Delta \left(\sum_{out}^{in} x_i \cdot m_i \right) = 0 \quad (19)$$

As for the path10, the density of 0.9999 for the dilution is considered. For calculating the amount of mass transfer inside the rectifier, “vmf” denotes the vapor mass fraction and “imf” represents the initial mass of fraction are required. They can be calculating as following:

$$vmf_{Rectifier} = \frac{x_4 - x_{13}}{x_{10} - x_{13}} \quad (20)$$

$$lmf_{Rectifier} = \frac{x_{10} - x_4}{x_{10} - x_{13}} \quad (21)$$

Then “vmf” and “imf” are used in another relationship to calculate the amount of mass transfer inside the rectifier. The temperature and the pressure are equal to those of path 13.

$$T_{10} = T_{13} = T_{Rectifier} \quad (22)$$

$$P_{10} = P_{13} = P_{max} \quad (23)$$

$$m_{10} = vmf_{rectifier} \times m_4 \quad (24)$$

$$m_{13} = lmf_{rectifier} \times m_4 \quad (25)$$

3.2.5. Path 7 (stream exiting the steam boiler and entering the super heater)

The weakened dilution which is separated in the rectifier has been heated to the point that is turned into vapor after passing through the boiler. Pressure is in its maximum state and the temperature is equal to the dilution temperature in boiler. Conditions under the state 7 are as follows:

$$T_7 = T_{Boiler} \quad (26)$$

$$P_7 = P_{max} \quad (27)$$

$$x_7 = x_{13} \quad (28)$$

$$m_7 = m_{13} \quad (29)$$

3.2.6. Path 8 (Turbine's inlet)

The weak ammonia dilution will have an extremely high temperature and can be considered to be super-hot after passing through the boiler and the super heater. The temperature is equal to the that in heat exchanger and the pressure is in its maximum state. In addition, the mass flow rate and the density of dilution are equal to those of the state 7. The conditions of the super heater are as follows:

$$T_8 = T_{Heat-Exchanger} \quad (30)$$

$$P_8 = P_{max} \quad (31)$$

$$x_8 = x_7 \quad (32)$$

$$m_8 = m_7 \quad (33)$$

3.2.7. Path 9 (turbine's output Stream)

The isentropic factor of the turbine can be obtained from Table 1. The turbine's outlet pressure is the minimum pressure of the combined cycle. And the density of the dilution at this stage is known in advance. Therefore, the conditions of turbine's exit stream can be evaluated via the following relationships:

$$P_9 = P_{min} \quad (34)$$

$$S_{isentropic} = S_8 \quad (35)$$

$$x_9 = x_8 \quad (36)$$

$$W_{Turbine} = m_8 \times (h_8 - h_9) \quad (37)$$

With these conditions, the isentropic enthalpy of expansion inside the turbine can be calculated. And the following equation is used to calculate the real enthalpy at the turbine's outlet point:

$$\eta_{Turbine} = \frac{h_8 - h_9}{h_8 - h_{isentropic}} \quad (38)$$

3.2.8. Path 1 (Condenser's outlet stream)

The enriched ammonia dilution is turned into liquid after passing through the condenser. The temperature is considered to be 5 °C higher than the ambient temperature and the density of 0.9999 is proposed. The Conditions of the state 1 are as follows:

$$P_1 = P_{max} \quad (39)$$

$$T_1 = T_0 + 5 \quad (40)$$

$$x_1 = 0.9999 \quad (41)$$

$$m_1 = m_{10} \quad (42)$$

3.2.9. Path 2 (evaporator's inlet stream)

Enriched dilution is reduced significantly by the pressure relief valve and reaches to a low pressure. Inside the valve, it is clear that the other conditions will be constant and the following conditions are existed.

$$h_2 = h_1 \quad (43)$$

$$P_2 = P_{min} \quad (44)$$

$$x_2 = x_1 \quad (45)$$

$$m_2 = m_1 \quad (46)$$

3.2.10. Path 3 (evaporators output Stream)

The enriched dilution is turned into liquid and its pressure is reduced to the minimum. And after passing through the evaporator and achieving the cooling effects of refrigeration, its temperature is 5 °C lower than the ambient temperature. Conditions at this point are as follows:

$$T_3 = T_0 - 5 \quad (47)$$

$$P_3 = P_{min} \quad (48)$$

$$x_3 = x_2 \quad (49)$$

In the following, streams 3 and 9 will be combined at the absorber. And after passing through this equipment, the base dilution is reformed. The following conditions hold at the absorber:

Table 1
Main assumptions for power and refrigeration combined cycle.

Ambient temperature	293.15	K
Ambient pressure	1.0135	Bar
Turbine's inlet pressure	25	Bar
Turbine's inlet temperature	558.15	K
Isentropic factor of the turbine	85	%
Refrigeration temperature	248.15	K
Temperature of the heat source	573.15	K
Mass rate of the heat source	20	kg/s
Pinch point temperature difference	288.15	K
Isentropic factor of the pump	70	%
Density of the ammonia base dilution	0.34	kg/m ³

$$\Delta \left(\sum_{out}^{in} m_i \right) = 0 \tag{50}$$

$$\Delta \left(\sum_{out}^{in} m_i \cdot h_i \right) + \Delta \left(\sum_{out}^{in} Q_j \right) + \Delta \left(\sum_{out}^{in} W_k \right) = 0 \tag{51}$$

$$\Delta \left(\sum_{out}^{in} x_i \cdot m_i \right) = 0 \tag{52}$$

3.3. Parametric analysis

The considered combined cycle can be heated up by using the exhaust of gas turbine [36], solar [37], geothermal [38] or other sources of heat. In this paper, the wasted heat of output gas streams which is composed of 96.41% of nitrogen, 3.59% of oxygen, 0.23% of water, 0.02% of NO and NO2 has been used as the heat source of the cycle. The main assumptions are presented in Table 1. The thermodynamic state of each status of combined refrigeration and power cycle is presented in Tables 2 and 3, respectively. Table 4 shows the results of thermodynamic simulation. The simulation is performed by using the EES software.

Parametric evaluation is used for studying the effects of parameters on the performance of the cycle suchlike ambient temperature, heat source temperature, inlet temperature, pressure of the turbine, refrigeration temperature, and the density of the ammonia base dilution. When a parameter is under investigation, then other parameters are kept as the constant values. The initial parameters are presented in Table 1.

As observed from the Fig. 2, the net power output is increased by the temperature of the heat source which is due to the fact that higher temperature of the heat source results in a higher inlet temperature of the turbine. And at the same time, it will cause an increment in steam flow rate that result in a higher net power output. In addition, the net power output is increased with a decrement in the density of ammonia based dilution which is due to the presence of ammonia in the dilution that passes through the turbine and causes a reduction in the power output.

Fig. 3 presents the effect of the heat source temperatures on the refrigeration output with varied densities of ammonia base dilution. It is obviously that the refrigeration output is increased by the increment of the heat source temperature. Even though, the input temperature from the evaporator is constant with the changes of the temperature of heat source. However, the increment of temperature of the heat source raises the mass flow rate of evaporator. Then it can be concluded that a higher density of ammonia base dilution will result in a higher refrigeration output which is due to the amount of dilution that passes through the evaporator. This reveals that higher amount of ammonia will result in a higher refrigeration output.

Fig. 4 presents the effects of the heat source temperatures on the exergy efficiency with different densities of ammonia dilution. As observed from this figure, the system’s exergy efficiency increases with the increment of heat source temperature. High temperature of the heat source increases the output power of the turbine and refrigeration rate. Therefore, based on the stated relationship for the exergy efficiency, its resulting efficiency is increased. In addition, higher density of ammonia based dilution yields higher energy efficiency which is due to the higher amount of ammonia passing through the evaporator. And finally, it will result in a higher refrigeration output and lower net power output.

As observed from the Fig. 5, the net power output is initially increased with the inlet pressure of the turbine, and then reduced. This is due to the fact that the reduction of enthalpy in the turbine with the increment in the pressure ratio is the main reason for the initial increment in the net power output. As the process continues, with a further increasing in the pressure ratio, the obtained enthalpy achieved

by the increment in pressure ratio is not sufficient to combat the reduction in vapour flow rate. Therefore, the net output power is reduced. Additionally, the net output power is reduced with an increment in the ambient temperature. This is due to the fact that the condensation temperature increases by absorbing the ambient temperature and results in the increasing of the pressure behind the turbine. Therefore, the increment in the pressure behind the turbine results in the reduction of net output power from the turbine.

It is evidently observed from the Fig. 6 that the refrigeration outlet is reduced with the increasing of the inlet pressure. The reason for this effect is the increment in turbine’s inlet pressure reduces the mass flow rate of evaporator. In other words, when the turbine’s inlet pressure is high, the mass flow rate of the whole cycle and the mass flow rate of the evaporator are reduced. The output refrigeration by the increment of the ambient temperature is then reduced. And the inlet pressure of the evaporator is also increased with the rising of the ambient temperature. Increment in the inlet temperature of the evaporator causes reduction in refrigeration output.

Fig. 7 shows the inlet pressure effect of the turbine on exergy efficiency at varied ambient temperatures. As it can be observed from this figure, the exergy efficiency is initially increased with a rise in inlet pressure of the turbine. Then it is reduced. Also, the exergy efficiency is reduced as the ambient temperature is increased.

Fig. 8 shows the temperature of refrigeration effects on the output of net power in different inlet temperatures of the turbine. As it can be observed from the figure, the net output power remains unchanging with the increment in refrigeration temperature. And at higher inlet temperatures of the turbine, a higher net output power is obtained. As changing in the refrigeration temperature is unable to affect the outlet and inlet conditions of the turbine, the net output power remains constant with changes to temperature of refrigeration. Additionally, higher inlet temperature of the turbine increases the power output of the turbine that results in generation of a higher net output power of the system.

Fig. 9 shows the effect of the refrigeration temperature on the refrigeration output at varied inlet temperatures of the turbine. Once a raise in the refrigeration temperature occurs, the refrigeration output consequently increases. And a higher inlet temperature of the turbine results in a lower refrigeration output. This will happen when the refrigeration temperature is extremely low and obtaining a high refrigeration outlet is difficult. It means that if we assume a lower refrigeration temperature, it will be difficult to achieve refrigeration and cooling at the assumed temperature. This is due to high evaporation rate of ammonia in the evaporator and the ambient temperature of its surroundings.

Fig. 10 shows the effect of the refrigeration temperature on the exergy efficiency in varied inlet temperatures of the turbine. This is

Table 2
Simulation results for power and refrigeration combined cycle.

Density	Mass flow rate (kg/s)	Entropy (kJ/kg K)	Enthalpy (kJ/kg)	Pressure (bar)	Temperature (K)	State
0.9999	0.193084	0.4134	118	25	298.15	1
0.9999	0.193084	0.5263	118	1.1941	243.1	2
0.9999	0.193084	5.295	1285	1.1941	268.15	3
0.34	1.46725	0.2738	-98.75	1.1941	298.15	4
0.34	1.46725	0.2711	-96.68	25	298.1	5
0.34	1.46725	2.5741	77.3	25	434.4	6
0.24	1.27416	6.222	2537	25	488.5	7
0.24	1.27416	6.571	2719	25	558.15	8
0.24	1.27416	6.8055	2235	1.1941	369.8	9
0.9999	0.386168	4.0323	1305.72	25	334.69	10
0.9999	0.193084	0.4134	118	25	298.15	11
0.24	0.026106	6.222	2537	25	488.5	12
0.24	1.30027	1.96341	538.8	25	434.4	13

Table 3
Simulation results for heat source fluid.

Molar Composition				Mass flow rate (kg/s)	Entropy (kJ/kg K)	Enthalpy (kJ/kg)	Temperature (K)	State
N ₂	O ₂	H ₂ O	NO + NO ₂					
0.9616	0.00359	0.0023	0.0002	20	7.41566	609.674	573.15	14
0.9616	0.00359	0.0023	0.0002	20	7.39417	597.473	562.398	15
0.9616	0.00359	0.0023	0.0002	20	7.13573	467.644	446.048	16
0.9616	0.00359	0.0023	0.0002	20	6.98558	405.083	388.678	17

Table 4
Performance of power and refrigeration cycle (all values are in kW).

Turbine's work	614.3
Pump's work	2.774
Heat taken by the absorber	3241
Heat taken by the condenser	458.59
Output refrigeration	225.5
Heat taken from the steam boiler	2612
Heat taken from the super heater	232.1
Heat taken from the heat exchanger	1282
Net power output	614.3
Net power and refrigeration output	839.8
Inlet temperature	41.27
Inlet exergy	1846.34
Heat efficiency (%)	20.35
Exergy efficiency (%)	35.68

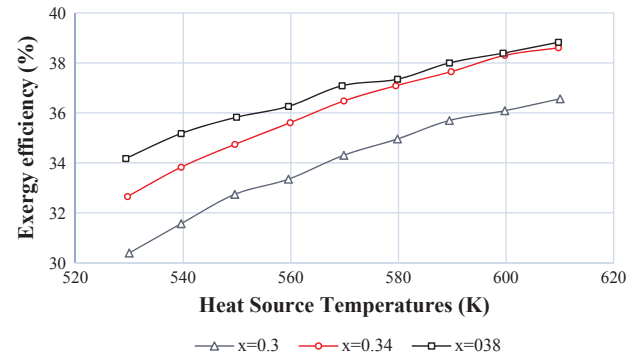


Fig. 4. Effect of Heat Source temperature on Exergy Efficiency according to Different Densities of Ammonia Base Dilution. X is the density of ammonia dilution.

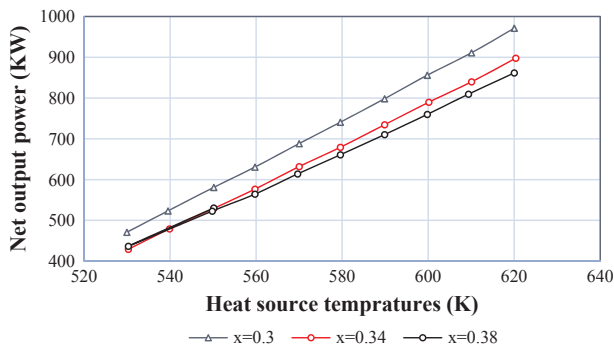


Fig. 2. Effects of Heat Source temperatures on the Net Power Output of the Turbine according to different densities of ammonia dilution. X is the density of ammonia dilution.

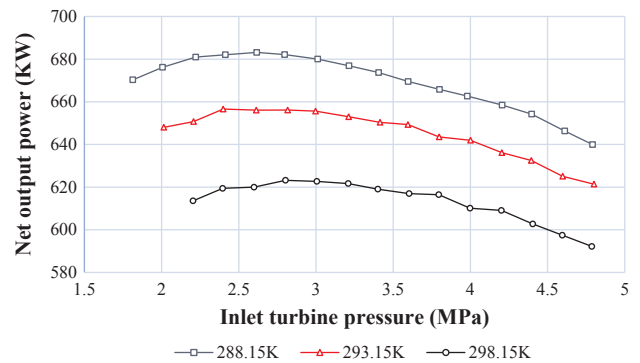


Fig. 5. Effect of Inlet Turbine Pressure on Net Output power at Different Ambient Temperatures. Environment temperature is shown in Kelvin.

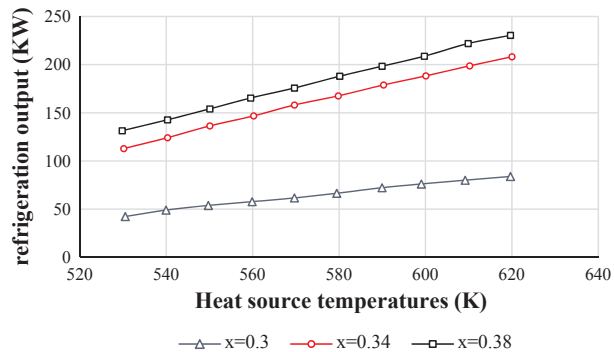


Fig. 3. Effects of Heat Source temperatures on the refrigeration Output of the Turbine according to Different Densities of Ammonia Dilution. X is the density of ammonia dilution.

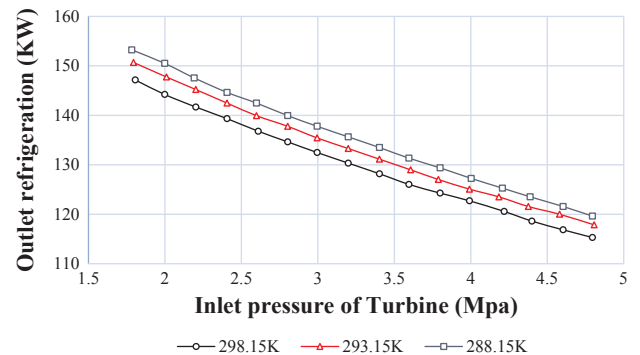


Fig. 6. Effect of Inlet Turbine Pressure on the refrigeration output at Different Ambient Temperatures. Environment temperature is shown in Kelvin.

evident from the fact that the exergy efficiency is reduced with an increment in refrigeration temperature. It means that as we assume a higher refrigeration temperature, a higher rate of cooling is obtained. And by considering the exergy equation, the exergy efficiency is further increased and a higher inlet temperature of the turbine results in a higher energy efficiency which is due to a higher power outlet from the

turbine.

In conclusion, it can be stated here that different parameters have variety of effects on the efficiency of the refrigeration and power combine cycle. And some of these parameters have an increasing effect whereas others have a reducing effect on the efficiency of this cycle. Therefore, according to the results of this study, the efficiency of this

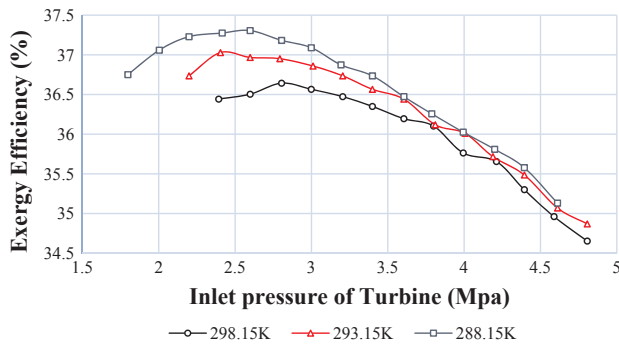


Fig. 7. Effect of Inlet Turbine Pressure on Exergy Efficiency at Different Ambient Temperatures. Inlet temperature of the turbine is shown in Kelvin.

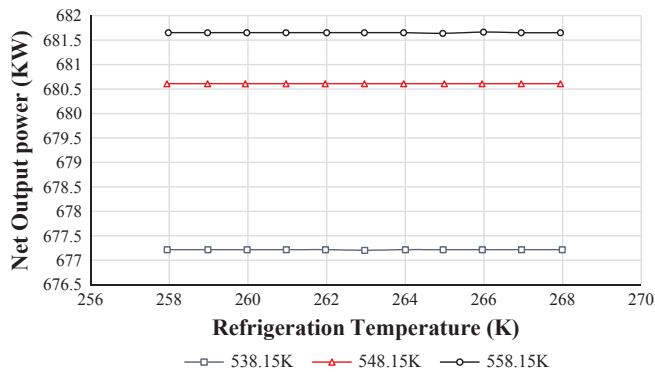


Fig. 8. Effect of Refrigeration Temperature on the Net Energy Efficiency at different inlet temperatures of the Turbine. Inlet temperature of turbine is shown in Kelvin.

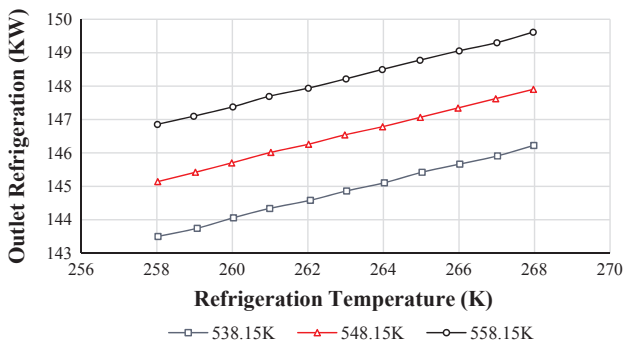


Fig. 9. Effect of Refrigeration Temperature on refrigeration output at Different Inlet Temperatures of the Turbine. Inlet temperature of the turbine is shown in Kelvin.

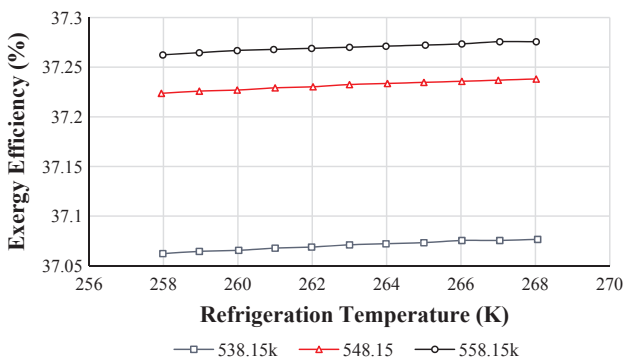


Fig. 10. Effect of Refrigeration Exergy Efficiency at Different Inlet Temperatures of the Turbine. Inlet temperature of the turbine is shown in Kelvin.

Table 5
Initial condition of optimization parameters.

Ambient temperature (K)	293.15
Ambient pressure (bar)	1.0135
Turbine's isentropic efficiency (%)	85
Refrigeration temperature (K)	268.15
Heat source temperature (K)	573.15
Mass flow rate of heat source (kg/s)	20
Pump's isentropic efficiency (%)	70
Temperature difference at the pinch point (K)	15
Turbine's inlet pressure range (bar)	15–40
Turbine's inlet temperature range (K)	538.15–560.15
Concentration range of ammonia base solution	0.26–0.38
Production stop	200
Population size	50
Incorporation probability	0.95
Mutation probability	0.05

Table 6
Optimization results for maximum net power output.

Turbine's inlet pressure (bar)	23.47
Turbine's inlet temperature (K)	558.1
Concentration of ammonia base solution	0.2801
Turbine's work (kW)	741.7
Pump's work (kW)	2.998
Outlet refrigeration (kW)	229.4
Net power output (kW)	738.7
Inlet exergy (kW)	1846.34
Thermal efficiency (%)	19.37
Exergy efficiency (%)	42.56

Table 7
Optimization result for maximum refrigeration output.

Turbine's inlet pressure (bar)	16.03
Turbine's inlet temperature (K)	558.1
Concentration of ammonia base solution	0.38
Turbine's work (kW)	700
Pump's work (kW)	37.07
Refrigeration output (kW)	304.4
Net power output (kW)	662.9
Inlet exergy (kW)	1846.34
Thermal efficiency (%)	22.76
Exergy efficiency (%)	39.88

Table 8
Optimization result for maximum thermal efficiency.

Turbine's inlet pressure (bar)	16.03
Turbine's inlet temperature (K)	558.1
Concentration of ammonia base solution	0.38
Turbine's work (kW)	718.8
Pump's work (kW)	37.09
Refrigeration output (kW)	304.4
Net power output (kW)	681.7
Inlet heat (kW)	4303
Inlet exergy (kW)	1846.34
Thermal efficiency (%)	22.92
Exergy efficiency (%)	40.09

cycle can be optimized which will be conducted in the next section.

4. Optimization by using the genetic algorithm

Parametric analysis has showed that the considered combined cycled in this study can be optimized. In order to obtain the maximum thermal efficiency and exergy efficiency, the genetic algorithm is used to conduct the optimization.

In this part, exergy efficiency and thermal efficiency is adopted to calculate the total performance of combined refrigeration and power

Table 9
Optimization result for maximum exergy output of the evaporator.

Turbine's inlet pressure (bar)	16
Turbine's inlet temperature (K)	553.4
Concentration of ammonia base solution	0.38
Turbine's work (kW)	712.8
Pump's work (kW)	37.24
Refrigeration output (kW)	304.4
Net power output (kW)	675.5
Inlet exergy (kW)	1846.34
Thermal efficiency (%)	22.87
Exergy efficiency (%)	40.57
Evaporator's exergy output (kW)	73.21

Table 10
Optimization result for maximum exergy efficiency.

Turbine's inlet pressure (bar)	16.03
Turbine's inlet temperature (K)	558.1
Concentration of ammonia base solution	0.28
Turbine's work (kW)	739.4
Pump's work (kW)	2.049
Refrigeration output (kW)	243.4
Net power output (kW)	737.3
Inlet exergy (kW)	1846.34
Thermal efficiency (%)	19.59
Exergy efficiency (%)	43.12

cycle. The first thermodynamic rule or thermal efficiency is as follows:

$$\eta_1 = \frac{W_{net} + Q_{ev}}{Q_{in}} \quad (53)$$

where W_{net} is the output power of turbine which is reduced by the input power to the pump. Q_{in} is the total heat which has been added to the cycle, Q_{eva} is the refrigeration output. The exergy efficiency is as follows

$$\eta_2 = \frac{W_{net} + Q_{ev}}{E_{in}} \quad (54)$$

where E_{in} is the heat source fluid exergy which is defined as follows:

$$E_{in} = m_g [(h_g - h_0) - T_0 (s_g - s_0)] \quad (55)$$

and E_{eva} exergy is related to refrigeration output. It is shown as follows:

$$E_{eva} = m_{eva} [(h_{eva,i} - h_{eva,0}) - T_0 (s_{eva,j} - s_{eva,0})] \quad (56)$$

In the software environment and programming, turbine's inlet temperature and pressure and the concentration of the ammonia base solution are chosen as the main variables where the inlet variables and other parameters are assumed to be constant. The reasons for selecting these three variables are their direct effect on the cycle. In other words, they tend to change the internal conditions of the cycle considerably whereas other parameters mainly relate to external conditions of the cycle. After numerical results are obtained, once the thermal efficiency and then the exergy efficiency of the cycle are calculated for optimization and obtainment of their maximum amount. Turbine's inlet temperature, pressure and the concentration of the ammonia based solution are selected as optimization variables.

Other parameters such as the refrigeration temperature, the heat source temperature, and ambient temperature are assumed to be constant. These limits are shown in Table 5. The objective functions are thermal and exergy efficiencies.

In order to obtain the maximum exergy and thermal efficiencies by using Eqs. (53) and (54), initially maxima of each part of these equations are calculated. Then these equations, i.e. exergy and thermal efficiencies, are optimized. The optimization is achieved by using the genetic algorithm and the results are presented.

In Table 5, initial optimization conditions are presented. Table 6 shows optimization results when the maximum net power output has been achieved. The maximum net power output is achieved when the

turbine's inlet pressure is 23.47 bars, its inlet temperature is 588.1 K, and the concentration ammonia base solution is at 0.2801. The net power output is 738.7 kW.

Table 7 shows the obtained results when the maximum outlet refrigeration has been achieved by the cycle. The maximum refrigeration output is obtained when the inlet pressure of the turbine is 16.03 bars, its inlet temperature is 558.1 K, and the concentration of ammonia base solution is 0.38. The refrigeration output is 304.4 kW. Table 8 presents the optimization results when the maximum thermal efficiency is achieved by the cycle. This is obtained when turbine's inlet pressure is 16.03 bar, inlet temperature of 558.1 K, and the concentration of ammonia base solution is 0.38. This is equivalent to 22.92 kW.

Table 9 presents the optimization results when the maximum exergy output from evaporator has been achieved. Maximum output of exergy in evaporator is achieved when turbine's inlet pressure is 16 bar, inlet temperature of 553.4 K, and the concentration of ammonia base solution is 0.38. It is equivalent to 73.21 kW.

Table 10 shows the results of optimization when the maximum exergy efficiency has been achieved. The maximum exergy efficiency is 43.12% while inlet pressure of turbine and temperature, and concentration of ammonia base solution are 16.07 bar, 558.1 K and 0.28 respectively. These results are approximately consistent with those results obtained from a similar cycle by Wang and his colleagues (reference). The differences are minimal between the present results and Wang's results. The reason for these differences are the use of equations for calculation the thermodynamic properties of binary mixture of ammonia-water.

5. Conclusion

The purpose of this research is to optimize a combined refrigeration and power cycle with different refrigerants by using the genetic algorithm. The considered cycle in this investigation applies a binary mixture of water and ammonia as its working fluid and is a combination of both absorption refrigeration and Rankine cycles. Parametric analysis of the thermodynamic parameters effects on the system performance shows that the temperatures of heat source, ambient, refrigeration the turbine as well as inlet pressure and the concentration of ammonia base solution (working fluid) have major effects on refrigeration output, the net output power, thermal, and exergy efficiencies. Parametric analysis also indicates that this combined cycle contains the conditions and potentials for optimization. And for this reason, this study implements the optimization of thermal parameters for obtaining the maximum exergy and thermal efficiencies as objective functions. Some results are summarized as follows:

1. Optimization is carried out by taking exergy and thermal efficiencies as the aim function via the genetic algorithm. The maximum thermal efficiency is 22.92% when the Inlet temperature and pressure of the turbine, and the concentration of ammonia base solution is 16.03 bar, 557.9 K and 0.38, respectively. The maximum exergy efficiency is 43.12% when the Inlet temperature and pressure of the turbine and the concentration of ammonia base solution are 16.03 bar, 558.1 K and 0.28, respectively.
2. Due to the structure and operating units such as evaporator, ejector and so on as well as optimal conditions, the considered cycle in this study can produce higher refrigeration when it is compared with the other combined power and refrigeration cycles.
3. Wang and colleagues [32] have only investigated on the exergy efficiency of the combined cycle. In contrast, this report has examined maximum refrigeration output, net power output, and thermal efficiency in addition to obtaining the maximum exergy efficiency. Wang and colleagues have used the El-sayed and Tribus [39] relations and the Ziegler [40] and Trip relationships for obtaining ammonia-water passes, whereas this research employs the EES Software with the other relationships such as the Ibrahim and

Klien [41] relation, a more accurate methodology than the ones used by Wang et al [32].

- For the considered cycle, only ammonia water mixture can be used in the combined power and refrigeration cycle amongst binary working fluids as refrigerants. As other fluids when divided to refrigerant and absorbent, the fluids have to act as the absorbent and to leave salty residues or sediments behind, once they pass through the turbine. For this reason, these fluids have no practical use in turbine.

Acknowledgment

This research investigation was supported by NSFC Funds (Nos. 11302069, 11372097), the 111 project under Grant B12032.

References

- Hossain SN, Bari S. Waste heat recovery from the exhaust of a diesel generator using Rankine Cycle. *Energy Convers Manage* 2013;75:141–51.
- Shen P, Lukes JR. Impact of global warming on performance of ground source heat pumps in US climate zones. *Energy Convers Manage* 2015;101:632–43.
- Kamal WA. Improving energy efficiency — the cost effective way to mitigate global warming. *Energy Convers Manage* 1997;38(1):39–59.
- Gogoi TK, Talukdar K. Thermodynamic analysis of a combined reheat regenerative thermal power plant and water–LiBr vapor absorption refrigeration system. *Energy Convers Manage* 2014;78(2):595–610.
- Maloney James D. Jr, Robertson RC. Thermodynamic study of ammonia-water heat power cycles. Thermodynamic study of ammonia-water heat power cycles; 1953.
- Kalina AI. Closure to “discussion of ‘combined-cycle system with novel bottoming cycle’”. *J Eng Gas Turb Power* 1985;107(4):1047–8.
- Chen Y, Han W, Jin H. Thermodynamic performance optimization of the absorption-generation process in an absorption refrigeration cycle. *Energy Convers Manage* 2016;126:290–301.
- Xu F, Goswami DY, Bhagwat SS. A combined power/cooling cycle. *Energy* 2000;25(3):233–46.
- Sarr JAR, Mathieu-Potvin F. Increasing thermal efficiency of Rankine cycles by using refrigeration cycles: a theoretical analysis. *Energy Convers Manage* 2016;121:358–79.
- Yang X, Zheng N, Zhao L, et al. Analysis of a novel combined power and ejector-refrigeration cycle. *Energy Convers Manage* 2016;108:266–74.
- Sun W, Yue X, Wang Y. Exergy efficiency analysis of ORC (Organic Rankine Cycle) and ORC-based combined cycles driven by low-temperature waste heat. *Energy Convers Manage* 2017;135:63–73.
- Mohtaram S, Chen W, Zargar T, et al. Energy-exergy analysis of compressor pressure ratio effects on thermodynamic performance of ammonia water combined cycle. *Energy Convers Manage* 2017;134:77–87.
- Mohtaram S, et al. Evaluating the effect of ammonia-water dilution pressure and its density on thermodynamic performance of combined cycles by the energy-exergy analysis approach. *Mechanics* 2017;23(2):209–19.
- Ahmadi GR, Toghraie D. Energy and exergy analysis of Montazeri Steam Power Plant in Iran. *Renew Sustain Energy Rev* 2016;56:454–63.
- Ahmadi Gholam reza, Toghraie Davood. Parallel feed water heating repowering of a 200 MW steam power plant. *J Power Technol* 2015;95(4):288–301.
- Ahmadi G, Toghraie D, Azimian A, et al. Evaluation of synchronous execution of full repowering and solar assisting in a 200 MW steam power plant, a case study. *Appl Therm Eng* 2017;112:111–23.
- Ahmadi Gholam Reza, Toghraie Davood, Akbari Omidali. Efficiency improvement of a steam power plant through solar repowering. *Int J Exergy* 2017;22(2):158–82.
- Ahmadi G, Toghraie D. Solar parallel feed water heating repowering of a steam power plant: a case study in Iran. *Renew Sustain Energy Rev* 2017;77:474–85.
- Keshavarz E, Toghraie D, Haratian M. Modeling industrial scale reaction furnace using computational fluid dynamics: a case study in Ilam Gas Treating Plant. *Appl Therm Eng* 2017;123:277–89.
- Akbari OA, Toghraie D, Karimipour A. Numerical simulation of heat transfer and turbulent flow of water nano fluids copper oxide in rectangular microchannel with semi-attached rib. *Adv Mech Eng* 2016;8(4).
- Alipour H, Karimipour A, Safaei MR, et al. Influence of T-semi attached rib on turbulent flow and heat transfer parameters of a silver-water nanofluid with different volume fractions in a three-dimensional trapezoidal microchannel. *Physica E* 2017;88:60–76.
- Multi-objective optimization of nano fluid flow in double tube heat exchangers for applications in energy systems. *Energy*; 2017.
- Sorour MM. Performance of a small sensible heat energy storage unit. *Energy Convers Manage* 1988;28(3):211–7.
- Kang X, Wang Y, Huang Q, et al. Study on direct-contact phase-change liquid immersion cooling dense-array solar cells under high concentration ratios. *Energy Convers Manage* 2016;128:95–103.
- Zheng D, Chen B, Qi Y, et al. Thermodynamic analysis of a novel absorption power/cooling combined-cycle. *Appl Energy* 2002;83(4):311–23.
- Kalina AI. Combined cycle and waste heat recovery power systems based on a novel thermodynamic energy cycle utilizing low-temperature heat for power generation. *Mech Eng* 1983;105(11). 104–104.
- Fallah M, Mahmoudi SMS, Yari M, et al. Advanced exergy analysis of the Kalina cycle applied for low temperature enhanced geothermal system. *Energy Convers Manage* 2016;108:190–201.
- Kalina AL, Leibowitz HM. Applying Kalina technology to a bottoming cycle for utility combined cycles. In: ASME 1987 international gas turbine conference and exhibition; 1987, V004T10A012.
- Zhang N, Cai R, Lior N. A novel ammonia-water cycle for power and refrigeration cogeneration. In: ASME 2004 international mechanical engineering congress and exposition; 2004. p. 183–96.
- Zhang Na, Lior N. Development of a novel combined absorption cycle for power generation and refrigeration. *J Energy Resour Technol – Trans ASME* 2007;129(3):254–65.
- Liu M, Zhang N. Proposal and analysis of a novel ammonia–water cycle for power and refrigeration cogeneration. *Energy* 2007;32(6):961–70.
- Wang J, Dai Y, Lin G. Parametric analysis and optimization for a combined power and refrigeration cycle. *Appl Energy* 2008;85(11):1071–85.
- Pouraghaie M, Atashkari K, Besarati SM, et al. Thermodynamic performance optimization of a combined power/cooling cycle. *Energy Convers Manage* 2010;51(1):204–11.
- Sarr JAR, Mathieu-Potvin F. Increasing thermal efficiency of Rankine cycles by using refrigeration cycles: a theoretical analysis[J]. *Energy Convers Manage* 2016;121:358–79.
- Chiou JS, Lin TM, She KY, et al. Enrichment of ammonia concentration from aqua-ammonia vapors by using 3A molecular sieve. *Energy Convers Manage* 2009;50(10):2665–9.
- Cao Y, Dai Y. Comparative analysis on off-design performance of a gas turbine and ORC combined cycle under different operation approaches. *Energy Convers Manage* 2017;135:84–100.
- Zare V, Hasanzadeh M. Energy and exergy analysis of a closed Brayton cycle-based combined cycle for solar power tower plants. *Energy Convers Manage* 2016;128:227–37.
- Franco A, Vaccaro M. A combined energetic and economic approach for the sustainable design of geothermal plants. *Energy Convers Manage* 2014;87:735–45.
- El-Sayed YM, Tribus M. Thermodynamic properties of water-ammonia mixtures theoretical implementation for use in power cycles analysis vol. I. ASME Publication AES; 1985.
- Ziegler B, Trepp C. Equation of state for ammonia-water mixtures. *Int J Refrig* 1984;7(2):101–6.
- Ibrahim OM, Klein SA. Absorption power cycles. *Energy* 1996;21(1):21–7.